ACS Catalysis

Research Article

pubs.acs.org/acscatalysis

Enhanced Two-Dimensional Dispersion of Group V Metal Oxides on Silica

Joseph T. Grant,[†] Carlos A. Carrero,[†] Alyssa M. Love,[†] René Verel,[§] and Ive Hermans*[,†,‡]

[†]University of Wisconsin—Madison, Department of Chemistry, 1101 University Avenue, Madison, Wisconsin 53706, United States

[‡]University of Wisconsin—Madison, Department of Chemical and Biological Engineering, 1415 Engineering Drive, Madison, Wisconsin 53706, United States

[§]ETH Zurich, Department of Chemistry and Applied Biosciences, Vladimir Prelog Weg 2, 8093 Zurich, Switzerland

Supporting Information

ABSTRACT: The catalytic performance of supported metal oxides is often controlled by their two- or three-dimensional dispersion. Silica, one of the popular inert supports, triggers the undesired formation of three-dimensional nanoparticles at significantly lower loadings than other conventional supports like Al_2O_3, TiO_2, Nb_2O_5, or ZrO_2. This observation has been ascribed to the lower reactivity of surface SiOH groups toward the precursor, compared to other metal hydroxyl groups on different supports. In this contribution, we show that by promoting amorphous silica with low amounts of sodium, the surface density of two-dimensional metal oxide species can be significantly enhanced to the same level as all other oxide supports previously reported in the literature. This effect is demonstrated for the case of supported vanadia using a variety of spectroscopic techniques (i.e., Raman, diffuse reflectance UV−vis, and ^{51}V-MAS NMR), as well as a catalytic activity study for the oxidative dehydrogenation of propane (ODHP), a structure-sensitive probe reaction. The propane consumption rate was found to increase linearly with the vanadium surface density while the propylene selectivity was not affected until a monolayer coverage of ca. 9 vanadia per nm^2 was surpassed. The method is also applicable to other group V metals (i.e., Nb- and Ta-oxide), opening new perspectives for supported metal oxides.

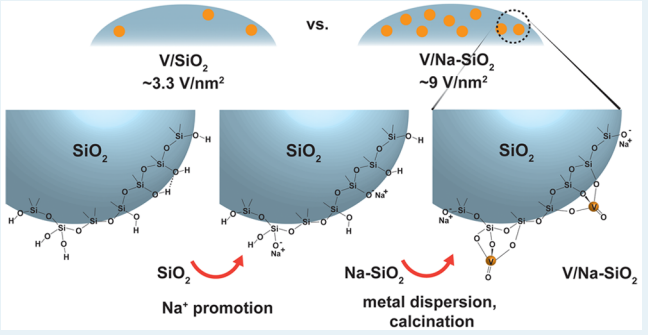

KEYWORDS: *supported metal oxides, metal oxide monolayer, oxidative propane dehydrogenation, vanadium oxide, metal oxide nanoparticles*

INTRODUCTION

Supported metal oxides are an important class of catalytic materials, used for a variety of important reactions such as alkane oxidation and olefin metathesis, among others.[1,2] The *surface structure* of such materials is known to control the catalytic performance.[3] Previous work in this area classified supported metal oxide structures as being above or below "monolayer coverage" defined as the maximum amount of two-dimensional (2D) metal oxide species that can exist on a support oxide surface before triggering the formation of three-dimensional (3D) nanoparticles.[4] Metal oxides below the monolayer exist solely as 2D "dispersed" surface structures and may be present as isolated monomers and/or oligo- or polymeric species, featuring one or more bridging oxygen atoms between the metal centers (M−O−M). Figure 1 compares monomeric and polymeric 2D structures with that of 3D nanoparticles of supported group V metal oxides.

The oxidative dehydrogenation of propane (ODHP) is a potential alternative for propane dehydrogenation (so-called "on-purpose" propylene production), due to its favorable thermodynamics and negligible coke formation. Yet, the low propylene selectivity restricts its industrial implementation, despite the potential for significant energy savings.[5,6] Though varieties of catalysts have been explored for ODHP,[7−13] supported vanadia catalysts have shown some of the most interesting results.[14−35] While the desired dehydrogenation

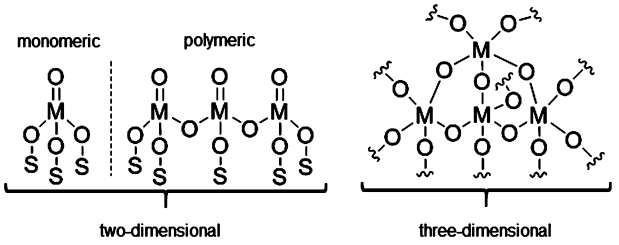

Figure 1. Two- (monomeric and oligomeric/polymeric) and three-dimensional group V supported metal oxide structures. S = support atom (Si, Al, Ti, etc.), M = supported metal (V, Nb, Ta).

Received: August 2, 2015
Revised: August 19, 2015
Published: August 24, 2015

DOI: 10.1021/acscatal.5b01679
ACS Catal. 2015, 5, 5787−5793

pathway is suggested to be structure-independent, the competing side-reactions, i.e. propylene (and to a lesser extent, propane) overoxidation to CO_x, becomes more favored over V_2O_5 nanoparticles.[15,35] Thus, in order to improve the propylene productivity, catalysts must maximize two-dimensional dispersion.

It is well established that the oxide support influences the catalytic activity, mainly due to intrinsic acid/base properties of the support.[35] Silica (SiO_2) is one of the most utilized oxide supports, due to its low cost and inert properties. However, up until now, SiO_2 only allows a low surface density of supported metal oxides to exist as 2D species compared to all other oxide supports, despite its high surface area. This is well documented in the case of supported vanadia (Figure 2), which can exist as

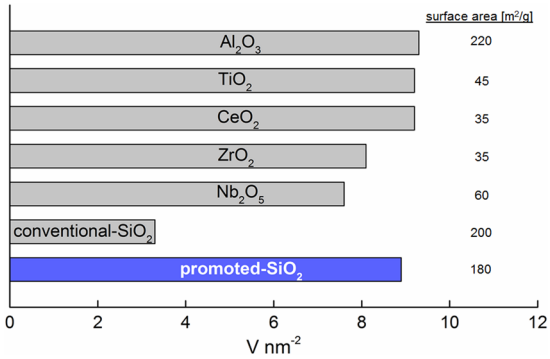

Figure 2. Experimental coverages of 2D vanadia species (in V nm^{-2}) on various oxide supports and their representative surface areas.[35]

2D species up to ~7−9 vanadium atoms per square nanometer (V nm^{-2}) on various oxide supports, except for SiO_2, which only allows up to 3.3 V nm^{-2},[35] irrespective of the synthesis protocol. This anomaly has previously been attributed to the low reactivity of surface hydroxyl groups on SiO_2,[36,37] resulting in less favorable vanadia anchoring to the SiO_2 surface. Greater metal oxide dispersion on SiO_2 could serve to increase the density of active sites, thus increasing the space-time yield, as well as to investigate synergetic effects between various surface species in close proximity (*viz.*, synergetic effects in combined monolayer materials).

In this study, we show that the optimal addition of sodium as a promoter can increase the level of dispersion of group V metal oxides on SiO_2 to be equivalent to that of other oxide support materials. This is demonstrated by a variety of characterization techniques, including Raman spectroscopy, diffuse reflectance UV−vis, and ^{51}V MAS NMR. Further, ODHP is utilized as a structure-sensitive probe reaction: increasing the 2D vanadia dispersion serves to linearly increase space-time yield while maintaining the same selectivity to propylene.

EXPERIMENTAL SECTION

Catalyst Preparation. Impure silica (*im*-SiO_2) was used as provided by the supplier (Sigma-Aldrich; 165 m^2 g^{-1}; batch #MKBN2949 V) without any further treatment. Na^+-promoted SiO_2 (*pro*-SiO_2) was prepared by incipient wetness impregnation of conventional amorphous silica (Aerosil200 from Evonik; 200 m^2 g^{-1}) by a sodium nitrate solution, followed by calcination under air. An appropriate amount of 1 M $Na(NO_3)$ solution was diluted in deionized H_2O to equal the pore volume of the Aerosil200 (1.3 mL g^{-1}). This sample was then calcined under air, ramping 1.5 °C min^{-1} to 700 °C, and holding at 700 °C for 4 h. The optimal *pro*-SiO_2 material contains 0.40 wt % Na^+ and shows a surface area of 180 ± 5 m^2 g^{-1}. Nitrate salts of alternative alkali or alkaline earth metals (Li-, K-, Rb-, Mg-nitrate) were used to attempt to substitute Na^+. Their methods of preparation are identical to that described for *pro*-SiO_2. The order of impregnation, whether it be V/alkali/support or alkali/V/support, and the consequences it may have on catalytic activity were previously studied.[38] This work suggested stronger alkali-support interaction with an initial alkali impregnation in case of alumina support. This resulted in more active vanadia species but did not address the influence on the metal oxide dispersion.

All supported metal oxide catalysts were synthesized via incipient wetness impregnation, following previously reported synthesis procedures for analogous materials.[39] Prior to impregnation, *im*-SiO_2, *pro*-SiO_2, or *conventional*-SiO_2 was dried under static conditions overnight at 120 °C. Impregnation was performed inside a glovebox under a dry N_2 atmosphere. Metal alkoxide solutions, *i.e.*, vanadium oxytriisopropoxide (VTI; Sigma-Aldrich), niobium ethoxide (Sigma-Aldrich, 99.95%), and tantalum ethoxide (Sigma-Aldrich, 99.98%), were used as the metal oxide precursors. Those alkoxide precursors were previously shown to be superior to other precursors like sodium metavanadate and the like.[15] The alkoxides were diluted with dry isopropanol (Sigma-Aldrich, 99.5%) or dry ethanol (Sigma-Aldrich, 99.5%) prior to impregnation to form a solution equal in volume to the pore volume of the support. The ratio of metal-to-isopropanol was altered to create a variety of metal oxide loadings. Impregnated samples were vacuum-dried inside the glovebox and transferred to a calcination oven where they were dried under a flow of N_2 at 120 °C for 3 h, ramped to 550 °C at 1 °C min^{-1} under dry air, and calcined at 550 °C for 3 h.

Catalyst Characterization. Raman measurements were carried out with a Renishaw InVia Raman Spectrometer with a 785 nm excitation laser. All measurements used a 1200 L mm^{-1} grating and were taken with a range of 250−1200 cm^{-1} and a dispersion of 1.36565 cm^{-1} $pixel^{-1}$. The experiments were performed in a high-temperature Linkam CCR1000 cell. Samples were dehydrated by heating to 500 °C (10 °C min^{-1} ramp) under 16 and 4 mL min^{-1} He and O_2, respectively, for 1 h before measurement.

Solid-state ^{51}V MAS NMR spectra were acquired on an Avance NMR spectrometer (Bruker, Karlsruhe, Germany) operating at a ^1H Larmor frequency of 400 MHz. The samples were spun around the magic angle with a rate of 18 kHz at room temperature using a double resonance 3.2 mm probe (containing ca. 15 mg sample). The probe was tuned to the resonance frequencies of ^{51}V (105.246 MHz). The parts per million scale of the spectra was calibrated using the ^{13}C signal of adamantane as an external secondary reference. Samples were dehydrated under a flow of dry air at 500 °C for 3 h prior to the NMR measurements.

Infrared spectra were recorded on a self-supporting wafer using a Bruker Alpha spectrometer in transmission mode (resolution of 2 cm^{-1}). The intensities were normalized to the Si−O−Si overtones of the silica framework. Diffuse reflectance UV−vis spectra were recorded with a Maya 200 spectrometer (Ocean Optics) equipped with a UV−vis deuterium/halogen light source (DH-2000-BAL from Mikropack) using $BaSO_4$ as a background. Both FT-IR and UV−vis analysis were carried out inside a glovebox (<1 ppm of H_2O and O_2).

DOI: 10.1021/acscatal.5b01679
ACS Catal. 2015, 5, 5787−5793

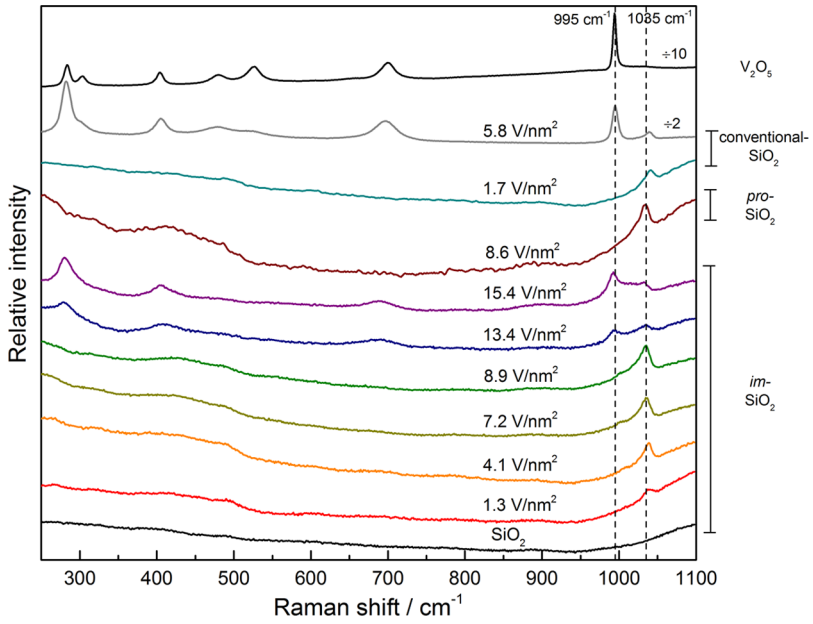

Figure 3. Raman spectra of dehydrated vanadia catalysts supported on *im*-SiO_2, *pro*-SiO_2, and conventional-SiO_2, compared to the Raman spectra of *im*-SiO_2 (bottom) and bulk V_2O_5 (top). Materials showing Raman features at 995, 700, 500, 400, and 300 cm^{-1} indicate the formation of V_2O_5 nanoparticles, while those only showing a band at 1035 cm^{-1} indicate supported two-dimensional vanadia species.

The point of zero charge (PZC) was determined according to a well-described method:[40] titration of 0.1 M HNO_3 to a blank reference solution (3 mL 0.1 M KNO_3, 2 mL 0.01 M KOH, 5 mL DI H_2O) and reference solution plus *conventional-* (or *pro-*) SiO_2 gradually lowered the pH of the solution. Intersection of the titration curves of the blank solution with that of the solution plus *conventional-* (or *pro-*)SiO_2 indicated the pH at which the quantity of $Si{-}OH_2^+$ sites was equivalent to that of $Si{-}O^-$ sites, defined as the PZC. The titration curves are displayed in the Supporting Information.

Vanadium loadings were determined using induced coupled plasma optical emission spectroscopy (ICP-OES) after complete acid digestion. Surface area and pore volume calculations were performed using Micromeritics 3-Flex instrumentation (t-plot analysis). Bulk analysis was repeated three times to accurately determine the metal oxide surface density. Details can be found in the Supporting Information.

ODHP Catalytic Activity. Catalytic activity measurements were performed using a Microactivity-Effi reactor. A total of 60−150 mg of catalyst (particle size of 600−710 μm) was mixed with inert SiC particles of equal size in a ratio of 2:1 (SiC-to-catalyst) and packed inside a quartz reactor tube (9 mm ID). Reactions were carried out at 490 °C with inlet flow ratios of 3:6:11 $O_2/C_3H_8/N_2$. Exhaust streams were analyzed using a Shimadzu 2010 GC equipped with three Restek columns (Rtx-1, Rt-Q-Bond, and RT-Msieve 5A) and a thermal conductivity detector (TCD) and flame ionization detector (FID). The catalysts were investigated under different contact times to monitor product selectivity at varying propane conversions (inverse weight-hour-space-velocity ($WHSV^{-1}$) of 20−140 [kg-cat s m^{-3}]). The carbon balance of each data point closes within 5%.

RESULTS AND DISCUSSION

From Serendipity to a Reproducible Synthesis Procedure. Use of impure SiO_2 (*im*-SiO_2) delivered directly from Sigma-Aldrich (batch #MKBN2949 V) allowed for a significantly better dispersion of vanadia than ever observed before. Indeed, V_2O_5 nanoparticles could not be detected up until a surface coverage as high as 8.9 V nm^{-2} (see below). Systematic addition of the various metal impurities found in *im*-SiO_2 (determined by ICP-OES) to conventional SiO_2 via incipient wetness impregnation (see Experimental section) revealed Na^+ to be the responsible promoter. The enhanced dispersion properties of *im*-SiO_2 could be reproduced by adding 0.40 wt % Na^+ using a 1 M $Na(NO_3)$ solution via incipient wetness impregnation to conventional-SiO_2 to create Na^+-promoted material (*pro*-SiO_2). Impregnation of vanadia to a SiO_2 support containing <0.40 wt % Na^+ did not show the enhanced dispersion effect (*viz.* formation of V_2O_5 particles), while impregnation of vanadia to SiO_2 material containing Na^+ loadings of ≥1.0 wt % revealed the formation of sodium metavanadate (Figure S1).

Surprisingly, when substituting sodium with other alkali or alkaline earth metals (Li^+, K^+, Rb^+, Mg^{2+}) with comparable promoter/V molar ratios, no enhanced 2D vanadia dispersion could be observed. Indeed, Raman spectroscopy reveals the formation of 3D V_2O_5 in almost all prepared samples (Figure S2). Catalysts containing higher amounts of promoter species show the emergence of unexpected Raman signals, distinct from that of supported V/SiO_2, likely due to the formation of a type of alkali-vanadate structure, similar to that detected for Na-metavanadate. It appears that sodium ions have the optimal properties to facilitate this unique dispersion enhancement.

Previous studies explored alkali-metal promoters for supported vanadium catalysts to neutralize acidic sites on various supports, and investigated its effect on the redox behavior.[41,42] It is worth emphasizing that in one study, the authors varied the molar ratio of Na/V between 0:1 and 1:1 for V/CeO_2 catalysts and monitored the effect on reducibility and activity for ODH of methanol.[43] At Na/V ratios <0.25, sodium addition only marginally decreased redox ability and showed no negative effect on catalytic activity, while the opposite is true with Na/V ratios >0.25.

DOI: 10.1021/acscatal.5b01679
ACS Catal. 2015, 5, 5787−5793

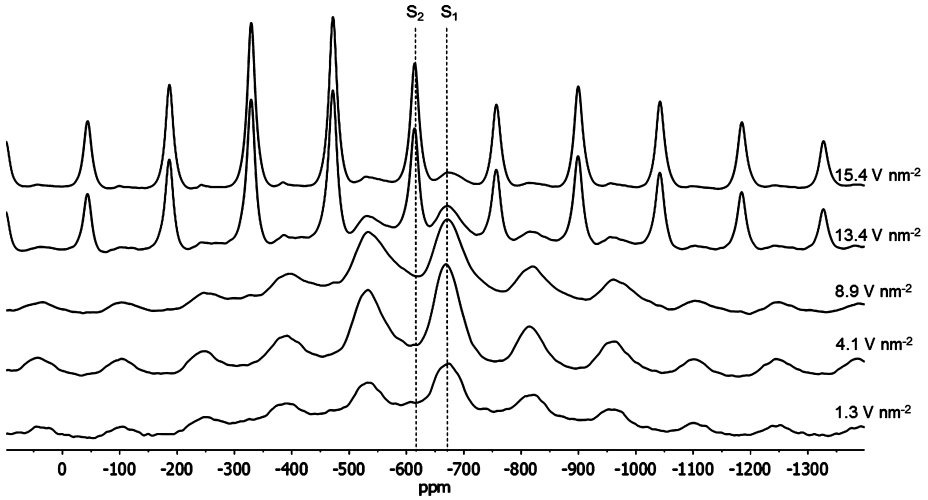

Figure 4. ^{51}V MAS NMR of dehydrated vanadia catalysts supported on *im*-SiO_2. Each catalyst shows an isotropic shift at −675 ppm (S_1), owing to the tetrahedral, monomeric vanadia species. Only catalysts above 8.9 V nm^{-2} show an additional isotropic shift at −614 ppm (S_2), attributed to the presence of 3D V_2O_5.

In this contribution, we focus on the effect of the Na^+-promoter on the structural properties of supported metal oxides on SiO_2 and couple this to the reactivity of the material using ODHP as a structure-sensitive probe reaction.

Enhancing 2D Dispersion. Raman spectra of the prepared materials are displayed in Figure 3. Under dehydrated conditions, each catalyst shows a Raman feature at 1035 cm^{-1}, assigned to V═O stretching of 2D vanadia species.[44,45] In agreement with previous Raman studies of supported vanadia on silica, vanadia supported on conventional SiO_2 shows the emergence of 3D V_2O_5 particles above a modest surface density of 1.7 V nm^{-2}. This is indicated by the appearance of a sharp signal at 995 cm^{-1}, as well as more broad features at 700, 530, 500, 400, and 300 cm^{-1}.[35] In the case of vanadia supported on *im*-SiO_2, these 3D V_2O_5 peaks do not appear at or below 8.9 V nm^{-2}, suggesting that a higher surface density of dispersed vanadia species can be obtained. With supported vanadia on *pro*-SiO_2, none of the 3D V_2O_5 peaks appear even with 8.6 V nm^{-2}. This result indicates that the enhanced dispersion properties of *im*-SiO_2 can be elegantly mimicked with the addition of 0.40 wt % Na^+ promoter.

It is important to note that the V═O stretching vibration of 2D vanadia at 1035 cm^{-1} does not shift to lower wavenumbers upon the addition of Na^+. This suggests that the V═O bond does not weaken upon Na^+ promotion as was observed in earlier work for higher Na^+ loadings.[42]

In addition to the Raman spectra, diffuse reflectance UV−vis (DRUV−vis) edge energy shifts of dehydrated vanadia catalysts supported on *im*-SiO_2 were determined (Figure S3). The edge energies of supported vanadia materials is an indicator of the V^{5+} ligand-to-metal charge transfer (LMCT) band, which shifts to lower energies with greater polymerization, due to greater electron delocalization in polymeric and 3D species.[2] All catalysts identified to contain only 2D vanadia via Raman characterization show edge energies between 3.30 and 3.40 eV. Meanwhile, catalysts with the highest vanadia surface density (i.e., 13.4 and 15.4 V nm^{-2}), containing 3D vanadia species as shown by Raman analysis, are characterized by lower edge energies between 2.28 and 2.60 eV. The literature assigns edge energies between 3.30 and 3.40 eV to isolated monomeric vanadia, while edge energies of 2.28−2.60 eV correspond to 3D nanoparticles.[2] Use of DRUV−vis edge energy analysis therefore corroborates our Raman spectroscopic assignments that 2D vanadia species can exist on Na^+-promoted SiO_2 up to 8.9 V nm^{-2}. No indication for polymeric species (edge energies around 3.0 eV) could be observed, in agreement with previous assertions that polymeric V−O−V species do not form on silica, in contrast to other supports.[36]

Solid-state ^{51}V MAS NMR spectra of dehydrated vanadia supported *im*-SiO_2 samples are displayed in Figure 4. Two distinct isotropic shifts are observed, effectively separating catalysts with and without 3D V_2O_5 nanoparticles. Here, the signal at −675 ppm, featuring many spinning side-bands, is assigned to the dispersed, monomeric VO_4 species.[46] The same isotropic shift appears in all investigated samples, regardless of the vanadia loading, suggesting the presence of analogous noninteracting species among these materials. The sharp signal appearing at −614 ppm is attributed to the distorted trigonal bipyramidal geometry of crystalline V_2O_5 and only appears for the samples containing the highest vanadia surface densities (i.e., 13.4 and 15.4 V nm^{-2}). This is in good agreement with previous works showing an isotropic shift of crystalline V_2O_5 at −612 ppm[47] and −610 ppm.[48] We emphasize that the V_2O_5 nanoparticles could not be detected with powder XRD, indicating that they must be very small in size. No NMR evidence could be found for the formation of oligomeric species, which is expected to show an isotropic shift at −350 ppm.[47] This observation is in agreement with our DRUV−vis results discussed above. Interestingly, the isotropic shift of the isolated vanadia species (i.e., −675 ppm) is slightly shifted compared to a $VO(OSiPh_3)_3$ reference (i.e., −720 ppm)[46] and compared to dispersed vanadia on unpromoted silica (*viz.*, −694 ppm, see Figure S4). This slight deshielding could point toward a weak (long distance) interaction of the vanadia with the sodium promotor.

The enhanced dispersion when using *im*-SiO_2 is not exclusive to supported vanadia but is also observed with the other group V metal oxides (i.e., niobium and tantalum oxides; see Raman spectra in Figure S5). Using conventional SiO_2, the maximum reported surface densities of supported Nb and Ta oxides were 1.1 Nb nm^{-2} and 0.8 Ta nm^{-2}, respectively.[44] When supported on *im*-SiO_2, these limits are expanded to at least 2.5 Nb nm^{-2}

DOI: 10.1021/acscatal.5b01679
ACS Catal. 2015, 5, 5787−5793

and 2.9 Ta nm^{-2} as the corresponding materials do not show Raman features of their respective 3D metal oxide species.

Catalytic Activity. The strong structure-sensitivity of ODHP can be conveniently used to characterize supported vanadium materials. When plotting the propylene selectivity as a function of propane conversion for the various catalysts (Figure 5), two different types of catalysts can be distinguished.

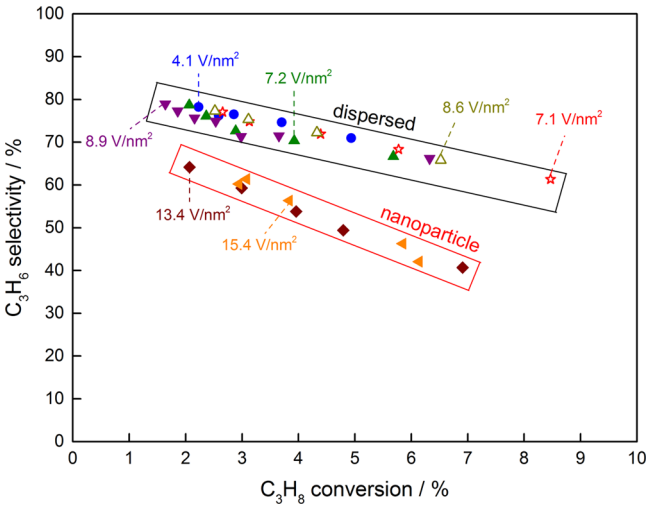

Figure 5. Propylene selectivity plotted as a function of propane conversion for vanadia catalysts supported on *im*- and *pro*-SiO_2. Catalysts containing V_2O_5 nanoparticles (*vide supra*) show a noticeable decrease in propylene selectivity compared to catalysts containing only 2D dispersed vanadia. Open symbols indicate *pro*-SiO_2 support material, while all others use *im*-SiO_2.

Indeed, the materials featuring V_2O_5 nanoparticles show an overall lower selectivity and a more rapid decrease of the selectivity as a function of conversion, pointing toward enhanced propylene combustion, in line with the literature data.[15,35]

In Figure 6, we show that the propane consumption rate is proportional to the vanadium surface density. We emphasize that the TOF, as well as the apparent activation energy of the submonolayer materials, is independent of the vanadium loading and in line with the reported data for V/SiO_2, i.e. (5.3 ± 0.7) × 10^{-3} s^{-1} and 116 ± 6 kJ mol^{-1}, respectively.[35] Coupled with the results in Figure 5, this indicates that the higher dispersion of vanadium results in a higher space-time yield, while not affecting the propylene selectivity. Previous work reported that alkali promoters significantly reduce the propane consumption TOF.[41,43] This effect is not noticed here when promoting SiO_2 with only 0.40 wt % Na^+ and is likely due to the low molar ratios of Na^+ to vanadium used in these *pro*-SiO_2 materials (<0.25 Na/V) compared to previous works (>1:1 Na/V). Also based on the ^{51}V-NMR results discussed above, it appears that the low amount of sodium does not significantly affect the molecular environment of the vanadia sites, only showing a minor deshielding of the vanadium by the sodium. This hypothesis is also in line with our observation that the catalytic activity of 5.6 wt % V supported on SiO_2 containing 2.2 wt % Na^+ (~1:1 Na:V) shows a 40% decrease in TOF (*viz.*, 3.1 × 10^{-3} s^{-1}) and is also associated with a lower propylene selectivity than that of 2D vanadia supported on *pro*-SiO_2 or *im*-SiO_2 (see Figure S6). The rate of propane consumption remains proportional to vanadium surface density, even with the emergence of 3D V_2O_5 above 9 V nm^{-2}. Considering this result, as well as the noticeable drop in selectivity upon formation of 3D V_2O_5 (Figure 5), the existence of 3D V_2O_5 appears to increase the rate of consecutive propylene combustion to CO_x.

Catalysts with high vanadia surface density remain stable for at least 4.5 days on stream, despite the high temperature and the formation of water as a reaction product. This is illustrated in Figure 7 for the case of 2D vanadia on *pro*-SiO_2 (8.6 V nm^{-2}), maintaining a stable propylene selectivity (66%) at 6.5% propane conversion. The spent catalyst was characterized using Raman to verify the absence of structural changes during the reaction. Neither Raman bands of 3D V_2O_5 nor those

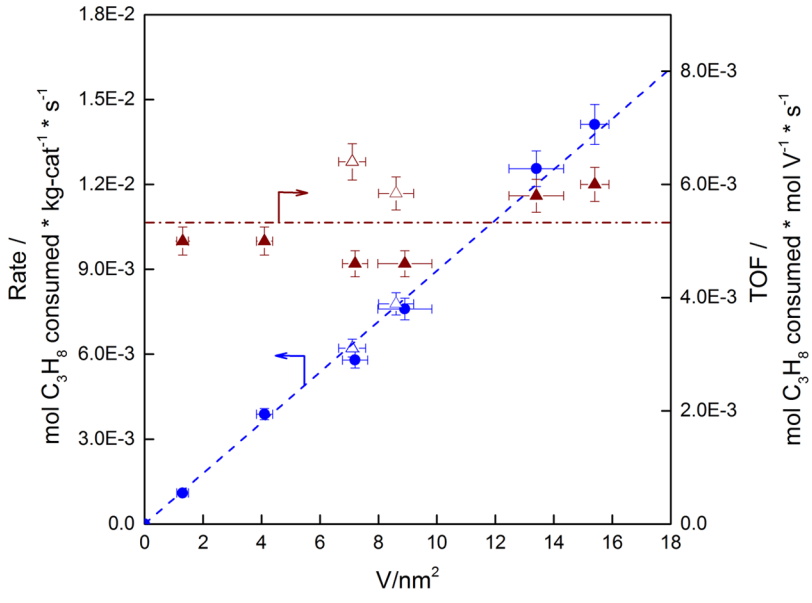

Figure 6. Rate of propane consumption (left-axis, blue data points) and TOF (right-axis, red data points) plotted as a function of the vanadium surface coverage. Open symbols (Δ) indicate *pro*-SiO_2 support material, while all others use *im*-SiO_2.

DOI: 10.1021/acscatal.5b01679
ACS Catal. 2015, 5, 5787−5793

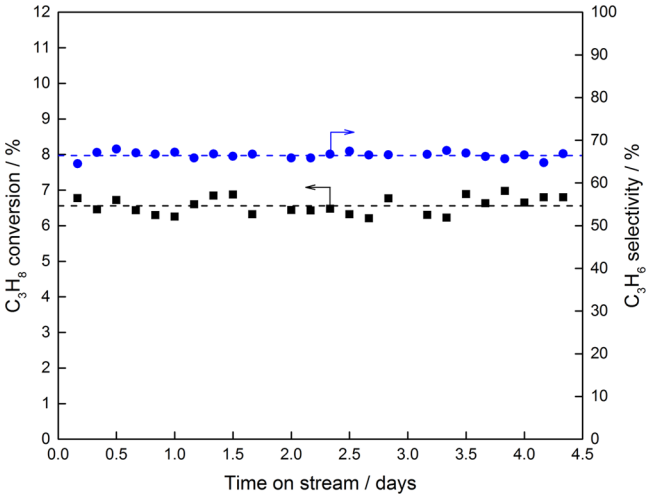

Figure 7. Catalytic activity of 8.6 V nm^{-2} supported on *pro*-SiO_2 for ODHP. Selectivity to propylene remains ~66% with ~6.5% propane conversion for at least 4.5 days on-stream. T = 490 °C, $WHSV^{-1}$ = 110 [kg-cat s m^{-3}].

corresponding to coke deposition could be observed (Figure S7).

Hypothesis for the Potential Role of Sodium As a Promoter. Metal oxide nanoparticles are formed when it becomes more favorable to anchor to supported metal oxide species rather than support-oxide anchoring sites during the impregnation and/or calcination. As a working hypothesis, we propose that Na^+ enhances 2D metal oxide dispersion on SiO_2 by exchanging with surface silanol groups, making these anchoring sites more reactive. This hypothesis is supported by IR spectroscopy (Figure S8), comparing spectra of dehydrated conventional-SiO_2 to *pro*-SiO_2. Sodium addition reduces the amount of silanol groups (features between 3745 and 3660 cm^{-1}) upon formation of more nucleophilic SiO^- species. This observation is also in line with the shift in the point of zero charge (PZC) from a pH of 4.4 to 6.3 upon the addition of sodium to Aerosil200 (Figure S9).

The highly nucleophilic ≡SiONa sites can more readily react with the $VO(O^iPr)_3$ precursor, yielding a surface bound ≡$SiO{-}V(O)(O^iPr)_2$ species plus NaO^iPr. The basic sodium isopropoxide could react with a less reactive silanol group, regenerating the more favorable ≡SiONa anchoring site. Our proposed (catalytic) mechanism for Na^+-assisted vanadium-oxide anchoring is displayed in Scheme 1. We envision that this mechanism could help in preferential multipodal bonding of the vanadium to the silica surface rather than atop surface-bound vanadium sites.

This proposed mechanism could also explain the necessity for an optimal amount of sodium to be present to observe enhanced 2D dispersion. It is indeed plausible that each silanol-activating Na^+ species can only migrate a limited distance before becoming surrounded by anchored vanadia species. No longer able to migrate via the proposed ion-exchange mechanism, vanadium-surrounded Na^+ species cannot activate the remaining unreactive silanol groups, leaving any unanchored $VO(O^iPr)_3$ precursor to anchor to already surface-bound vanadia during the calcination step, thus forming 3D V_2O_5. No evidence for the formation of VONa bonds could be found in the calcined materials, and ^{51}V NMR indicates only a slight downfield shift of the $(SiO)_3V{=}O$ vanadia centers upon the addition of sodium. Attempts to capture this effect using ^{23}Na MAS NMR with *pro*-SiO_2 catalysts have been unsuccessful to date due to the low signal-to-noise ratio, likely caused by (1) the low sodium content and, more importantly, (2) the amorphous nature of the support leading to peak broadening. The proposed hypothesis will be further investigated, also to explore why it is that other alkali and alkali-Earth metal ions (Li^+, K^+, Rb^+, Mg^{2+}) do not display the same enhanced 2D dispersion effect that Na^+-promoted SiO_2 offers. Most likely, sodium ions present an optimal balance between charge density and solvation by the isopropanol solvent used during the impregnation.

Scheme 1. Proposed Mechanism for the Activation of Silanol Groups by Na^+ and the Associated Migration of the Na^+ over the Support Surface

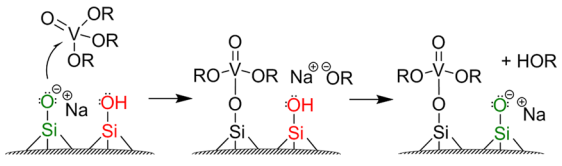

CONCLUSIONS

Structural properties of supported metal oxides, particularly the presence of 2D or 3D metal oxide species, control their catalytic performance. Out of all traditional oxide supports, SiO_2 has historically allowed the lowest 2D metal oxide dispersion, despite its high surface area. Using Raman and DR-UV−vis spectroscopy, ^{51}V-NMR, and catalytic activity data with ODHP as a probe reaction, we now show that the promotion of conventional silica with 0.40 wt % Na^+ can significantly enhance the dispersion of vanadia on SiO_2 to levels equivalent to that of other common oxide supports (i.e., up to 8.9 V nm^{-2}). Increasing the quantity of 2D vanadia serves to proportionally increase the rate of propane ODH while maintaining high propylene selectivity. Raman spectroscopy further confirms enhanced dispersion of the other group V metal oxides (Nb, Ta oxide) on Na^+-promoted SiO_2. It is hypothesized that the role of Na^+ is to ion-exchange with surface silanols to form more-reactive $Si{-}O^-Na^+$ anchoring sites. The silanol groups that would normally remain unreactive toward the metal oxide precursor now have the ability to function as an anchoring site. From the optimal Na/V ratio of 0.2, and the fact that the sodium promotion nearly triples the amount of dispersed vanadia, we propose a catalytic mechanism in which one sodium ion is able to facilitate the anchoring of several vanadia species. The enhanced metal oxide dispersion effect is displayed here for the case of group V metal oxides but likely includes other metal oxides as well. This finding presents exciting new opportunities for metal oxide catalysts supported on SiO_2.

ASSOCIATED CONTENT

Supporting Information

The Supporting Information is available free of charge on the ACS Publications website at DOI: 10.1021/acscatal.5b01679.

Figures S1−S9, equations, Table S1 (PDF)

AUTHOR INFORMATION

Corresponding Author

*E-mail: hermans@chem.wisc.edu.

DOI: 10.1021/acscatal.5b01679
ACS Catal. 2015, 5, 5787−5793

Notes

The authors declare no competing financial interest.

■ ACKNOWLEDGMENTS

The authors acknowledge financial support from the University of Wisconsin—Madison, as well as the Wisconsin Alumni Research Foundation (WARF).

■ REFERENCES

(1) Hu, J.; Chen, L.; Richards, R. In *Metal Oxide Catalysis*; Jackson, S. D., Hargreaves, J. S. J., Eds.; Wiley-VCH Verlag GmbH & Co. KGaA: Weinheim, Germany, 2009; pp 613−661.
(2) Chatzidimitriou, A.; Bond, J. Q. *Green Chem.* **2015**, *17*, 4367−4376.
(3) Tian, H.; Ross, E. I.; Wachs, I. E. *J. Phys. Chem. B* **2006**, *110*, 9593−9600.
(4) Russell, A.; Stokes, J. *Ind. Eng. Chem.* **1946**, *38*, 1071−1074.
(5) Ren, T.; Patel, M.; Blok, K. *Energy* **2006**, *31*, 425−451.
(6) Cavani, F.; Ballarini, N.; Cericola, A. *Catal. Today* **2007**, *127*, 113−131.
(7) Pless, J.; Bardin, B.; Kim, H.; Ko, D.; Smith, M. T.; Haammond, R. R.; Stair, P. C.; Poeppelmeier, K. R. *J. Catal.* **2004**, *223*, 419−431.
(8) Zhao, Z.; Gao, X.; Wachs, I. E. *J. Phys. Chem. B* **2003**, *107*, 6333−6342.
(9) Yuan, L.; Bhatt, S.; Beaucage, G.; Guliants, V. V.; Mamedov, S.; Soman, R. S. *J. Phys. Chem. B* **2005**, *109*, 23250−23254.
(10) Zhai, Z.; Wang, X.; Licht, R.; Bell, A. T. *J. Catal.* **2015**, *325*, 87−100.
(11) Vajda, S.; Pellin, M. J.; Greeley, J. P.; Marshall, C. L.; Curtiss, L. A.; Ballentine, B. A.; Elam, J. W.; Catillon-Mucherie, C.; Redfern, P. C.; Mehmood, F.; Zapol, P. *Nat. Mater.* **2009**, *8*, 213−216.
(12) Frank, B.; Zhang, J.; Blume, R.; Schlogl, R.; Su, D. S. *Angew. Chem., Int. Ed.* **2009**, *48*, 6913−6917.
(13) Sui, Z. J.; Zhou, J. H.; Dai, Y. C.; Yuan, W. K. *Catal. Today* **2005**, *106*, 90−94.
(14) Schwarz, O.; Habel, D.; Ovsitser, O.; Kondratenko, E. V.; Hess, C.; Schomaeker, R.; Schubert, H. *J. Mol. Catal. A: Chem.* **2008**, *293*, 45−52.
(15) Carrero, C. A.; Keturakis, C.; Orrego, A.; Schomaeker, R.; Wachs, I. E. *Dalton Trans.* **2013**, *42*, 12644−12653.
(16) Kondratenko, E. V.; Cherian, M.; Baerns, M. *Catal. Today* **2006**, *112*, 60−63.
(17) Kondratenko, E. V.; Cherian, M.; Baerns, M.; Schloegl, R.; Wang, X.; Wachs, I. E.; Su, D. *J. Catal.* **2005**, *234*, 131−142.
(18) Testova, N. V.; Shalygin, A. S.; Kaichev, V. V.; Glazneva, T. S.; Paukshtis, E. A.; Parmon, V. N.; *Appl. Catal., A*, **2015**, http://dx.doi.org/10.1016/j.apcata.2015.05.018. DOI: 10.1016/j.apcata.2015.05.018.
(19) Takehira, K.; Ohishi, Y.; Shishido, T.; Kawabata, T.; Takaki, K.; Zhang, Q.; Wang, Y. *J. Catal.* **2004**, *224*, 404−416.
(20) Shishido, T.; Shimamura, K.; Teramura, K.; Tanaka, T. *Catal. Today* **2012**, *185*, 151−156.
(21) Chen, K.; Bell, A. T.; Iglesia, E. *J. Phys. Chem. B* **2000**, *104*, 1292−1299.
(22) Argyle, M. D.; Chen, K.; Bell, A. T.; Iglesia, E. *J. Catal.* **2002**, *208*, 139−149.
(23) Malleswara Rao, T. V.; Deo, G. *AIChE J.* **2007**, *53*, 1538−1549.
(24) Dinse, A.; Frank, B.; Hess, C.; Habel, D.; Schomaeker, R. *J. Mol. Catal. A: Chem.* **2008**, *289*, 28−37.
(25) Grabowski, R. *Appl. Catal., A* **2004**, *270*, 37−47.
(26) Schwarz, O.; Duong, P.; Schaefer, G.; Schomaeker, R. *Chem. Eng. J.* **2009**, *145*, 420−428.
(27) Frank, B.; Dinse, A.; Ovsitser, O.; Kondratenko, E. V.; Schomaeker, R. *Appl. Catal., A* **2007**, *323*, 66−76.
(28) Rozanska, X.; Fortrie, R.; Sauer, J. *J. Am. Chem. Soc.* **2014**, *136*, 7751−7761.
(29) Dai, G. L.; Li, Z. H.; Lu, J.; Wang, W. N.; Fan, K. N. *J. Phys. Chem. C* **2012**, *116*, 807−817.
(30) Rozanska, X.; Fortrie, R.; Sauer, J. *J. Phys. Chem. C* **2007**, *111*, 6041−6050.
(31) Alexopoulos, K.; Reyniers, M. F.; Marin, G. *J. Catal.* **2012**, *289*, 127−139.
(32) Hofmann, A.; Ganduglia-Pirovano, M. V.; Sauer, J. *J. Phys. Chem. C* **2009**, *113*, 18191−18203.
(33) Popa, C.; Ganduglia-Pirovano, M. V.; Sauer, J. *J. Phys. Chem. C* **2011**, *115*, 7399−7410.
(34) Schimmoeller, B.; Jiang, Y.; Pratsinis, S. E.; Baiker, A. *J. Catal.* **2010**, *274*, 64−75.
(35) Carrero, C. A.; Schloegl, R.; Wachs, I. E.; Schomaecker, R. *ACS Catal.* **2014**, *4*, 3357−3380.
(36) Gao, X.; Bare, S. R.; Weckhuysen, B. M.; Wachs, I. E. *J. Phys. Chem. B* **1998**, *102*, 10842−10852.
(37) Wachs, I. E. *Catal. Today* **1996**, *27*, 437−455.
(38) Wang, X.; Wachs, I. E. *Catal. Today* **2004**, *96*, 211−222.
(39) Buyevskaya, O.; Bruckner, A.; Kondratenko, E.; Wolf, D.; Baerns, M. *Catal. Today* **2001**, *67*, 369−378.
(40) Bourikas, K.; Vakros, J.; Kordulis, C.; Lycourghiotis, A. *J. Phys. Chem. B* **2003**, *107*, 9441−9451.
(41) Lemonidou, A. A.; Nalbandian, L.; Vasalos, I. *Catal. Today* **2000**, *61*, 333−341.
(42) Garcia Cortez, G.; Fierro, J. L. G.; Banares, M. A. *Catal. Today* **2003**, *78*, 219−228.
(43) Li, Y.; Wei, Z.; Sun, J.; Gao, F.; Peden, C. H. F.; Wang, Y. *J. Phys. Chem. C* **2013**, *117*, 5722−5729.
(44) Lee, E. L.; Wachs, I. E. *J. Phys. Chem. C* **2007**, *111*, 14410−1442.
(45) Wu, Z.; Kim, H. S.; Stair, P. C. In *Metal Oxide Catalysis*; Jackson, S. D., Hargreaves, J. S. J., Eds.; Wiley-VCH Verlag GmbH & Co. KGaA: Weinheim, Germany, 2009; pp 177−194.
(46) Feher, F. J.; Blanski, R. L. *J. Am. Chem. Soc.* **1992**, *114*, 5886−5887.
(47) McGregor, J. In *Metal Oxide Catalysis*; Jackson, S. D., Hargreaves, J. S. J., Eds.; Wiley-VCH Verlag GmbH & Co. KGaA: Weinheim, Germany, 2009; pp 195−242.
(48) Hu, J. Z.; Xu, S.; Li, W.; Hu, M. Y.; Deng, X.; Dixon, D. A.; Vasiliu, M.; Craciun, R.; Wang, Y.; Bao, X.; Peden, C. H. F. *ACS Catal.* **2015**, *5*, 3945−3952.

DOI: 10.1021/acscatal.5b01679
ACS Catal. 2015, 5, 5787−5793